Electrical and Electronic Engineering 2012, 2(3): 88-95
DOI: 10.5923/j.eee.20120203.01

# Radiation Characteristics of Cylindrical Dielectric Resonator Antenna Mounted on Superquadric Cylindrical Body

**S.H. Zainud-Deen[1], Noha A. El-Shalaby[2,*], K.H. Awadalla[1]**

[1]Faculty of Electronic Engineering, Menoufia University, Menoufia, 32952, Egypt
[2]Faculty of Engineering, Kafrelsheikh University, Kafrelsheikh, 3317, Egypt

**Abstract** Characteristics of cylindrical dielectric resonator antenna on (CDRA) on superquadric cylindrical body are discussed in this paper. Curvature effects on radiation characteristics in different planes of (CDRA), the reflection coefficient, the input impedance, The co-polarization and the cross-polarization characteristics, gain of the antenna, are calculated and discussed for different values of ν "squareness parameter". Then show effect of changing the aspect ratio B/A on the reflection coefficient and the input impedance. The proposed antennas are numerically investigated using finite element method and the finite integration technique.

**Keywords** DRA, CDRA, FEM, FIT

## 1. Introduction

The dielectric resonator antenna (DRA) concept was first proposed in 19. Many practical applications of DRA mounted on planar surfaces were demonstrated[1-7]. DRA can be of any shape, but in practical applications, rectangular and cylindrical shapes are most common. Because of its simple geometry, DRA offers many advantages, such as low loss, easy of excitation, small size and broad beam characteristics. Recently, the radiation characteristics of cylindrical DRA mounted on or embedded in circular cylindrical ground plane are investigated[8,9].

In this paper, for the first time (to the best of our knowledge), CDRA mounted on superquadric cylindrical ground plane is implemented. Superquadrics are a powerful family of parametric shapes that allow complex solids and surfaces to be constructed and altered easily from a small number of interactive parameters. This kind of antennas can be of great interest for applications on the bodies of missiles, aircrafts and spacecrafts that have no planar surfaces on portions of their bodies. The finite element method (FEM)[10,11] is used to calculate the reflection coefficient, the input impedance, impedance bandwidth, and copolarized and cross-polarized field components in different planes. The metallic ground plane is assumed to be perfect conductor and the thickness is neglected since it is much less than that of the operating wavelength. The calculated results are validated using the finite integration technique (FIT)[12,13].

* Corresponding author:
noha1511ahm@yahoo.com (Noha A. El-Shalaby)
Published online at http://journal.sapub.org/eee


## 2. Antenna Structure

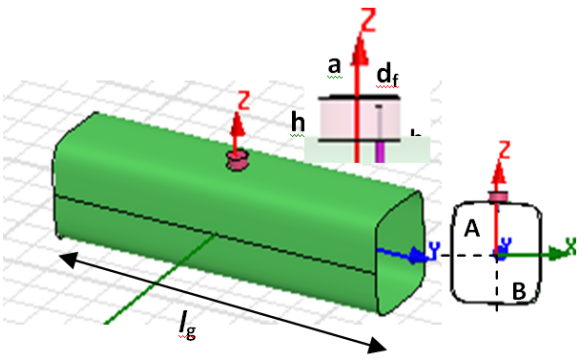


**Figure 1.** The geometry of CDRA mounted on superquadric cylinder ground plane structure for ν= 4

Fig.1 shows the geometry of CDRA mounted on ground superquadric cylindrical structure. The superquadric cross section curve of the cylinder is the locus of points satisfying the following equation (1)[14,15],

$$\left(\frac{x}{A}\right)^{\nu}+\left(\frac{y}{B}\right)^{\nu}=1 \qquad x \le A, \quad and \quad y \le B \tag{1}$$

Where "A" and "B" are the semi-axes in the x and y directions respectively, and ν is a "squareness parameter" which controls the behaviour of loop radius of curvature. The coordinates of any point on the curvature are given (2),

$$\left.\begin{aligned} X &= A\psi(\beta)\cos\beta \\ Y &= B\psi(\beta)\sin\beta \end{aligned}\right\} \tag{2}$$

Where

$$\psi(\beta) = \left(|\sin\beta|^{\nu} + |\cos\beta|^{\nu}\right)^{-1/\nu}$$

The parameter β is in the range (0≤β≤2π). An important feature of this particular representation is the fact that equal divisions in the parameter β results in reasonably equal values of arc length for the sub- different antenna configurations through the variation of parameters A, B, and ν starting from circular (ellipse) to square (rectangular) cross sectional area. The CDRA with dielectric constant $\varepsilon_r$ =12 is used. It has radius "a", of 2.75cm and a height "h", of 2.6 cm.

A coaxial probe with radius of 1.295 mm excites the antenna. The probe is located off the centre by $d_f$ =1.4 cm with a height "$h_f$", of 2cm.

## 3. Numerical Results

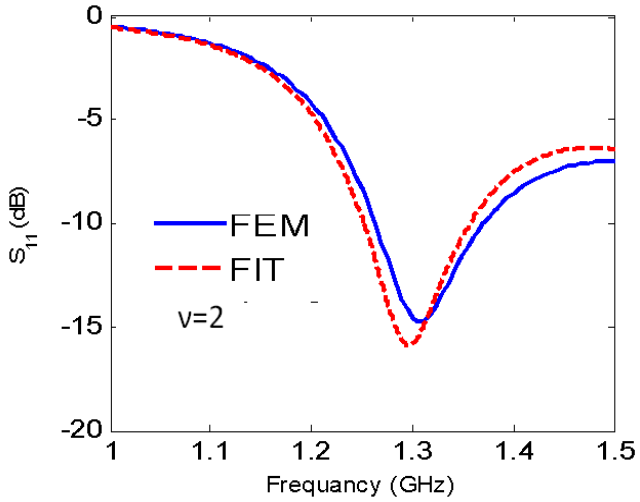


**Figure 2.** Reflection coefficient versus Frequency for lg = 50cm, A = B =12.5cm

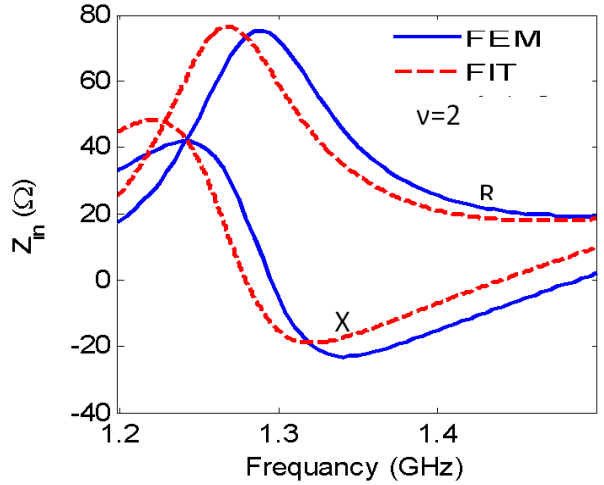


**Figure 3.** Input impedance versus frequency for lg= 50cm, A = B =12.5cm

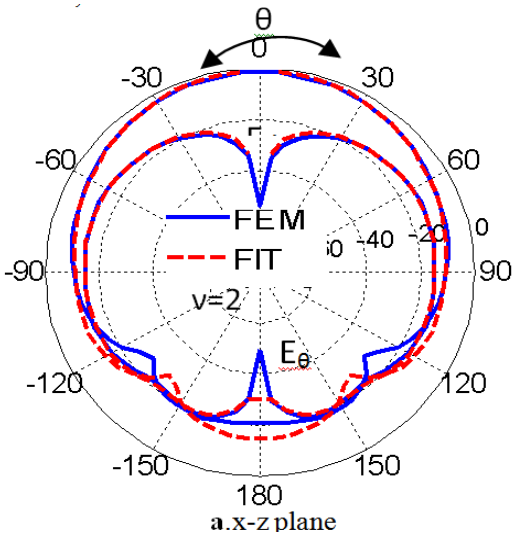


**Figure 4.** The radiation patterns in different planes at f = 1.305GHz

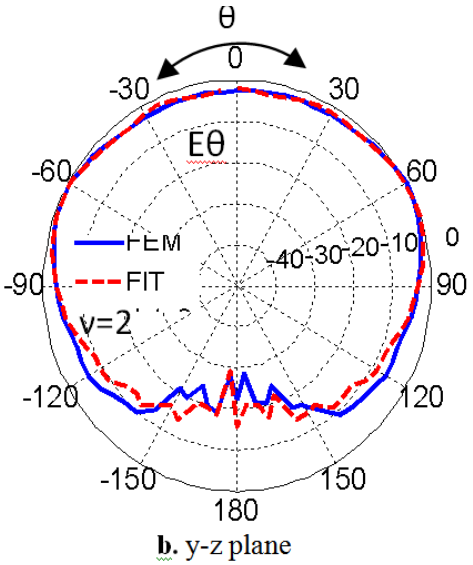


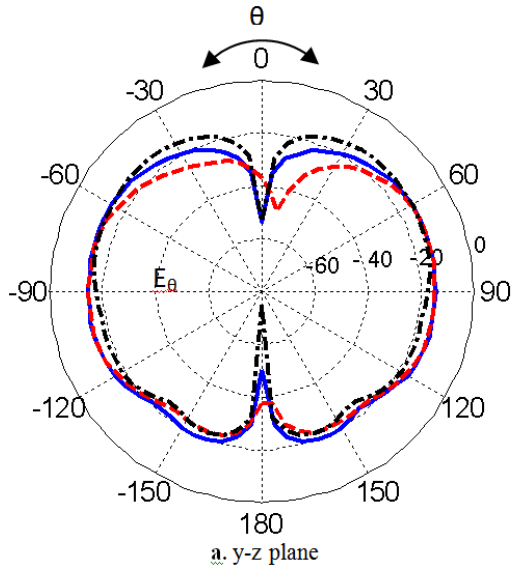

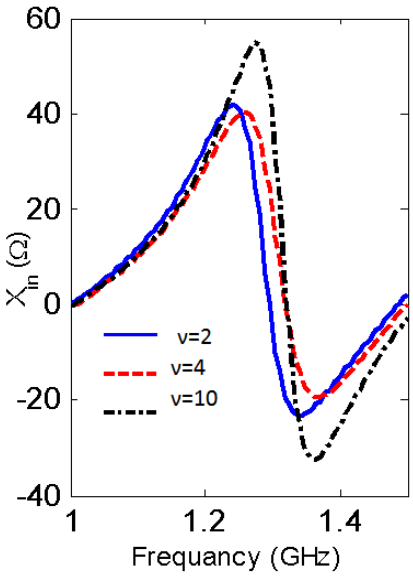


**b.** Input reactance.

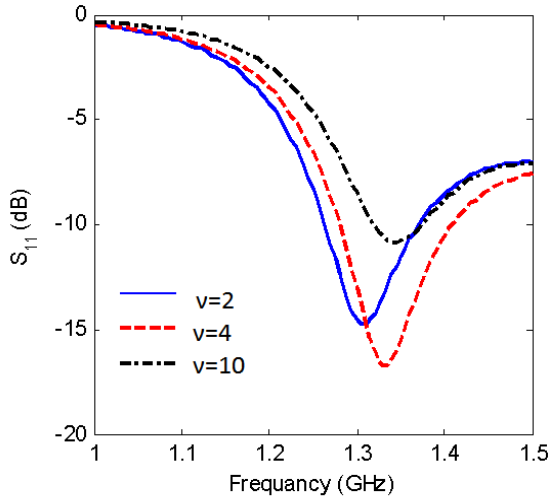


**c.** Reflection coefficient.

**Figure 5.** The reflection coefficient and input impedance versus the frequency for A =B=125 mm at different values of ν

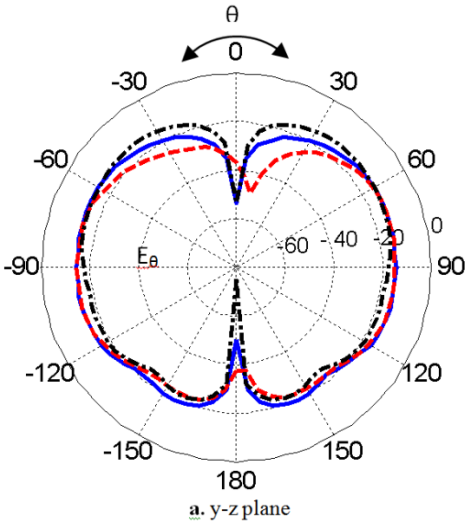


**a.** y-z plane

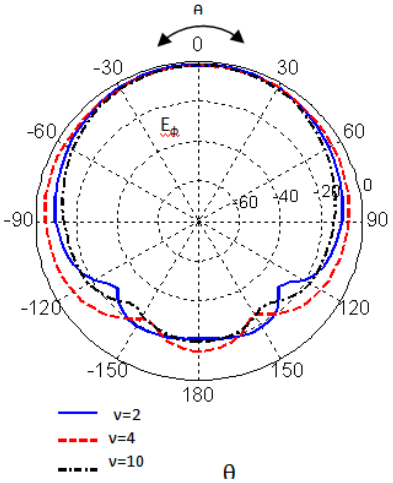


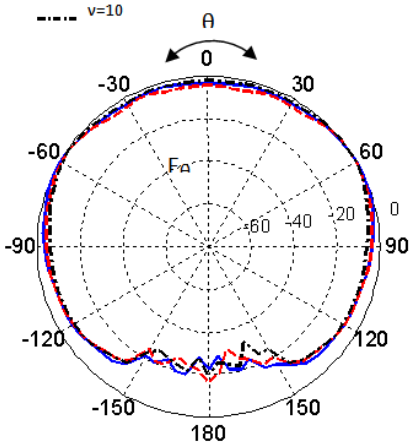


**b.** x-z plane

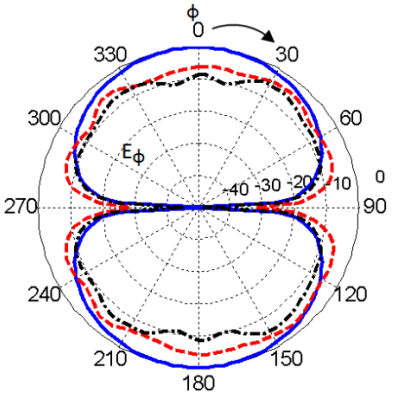


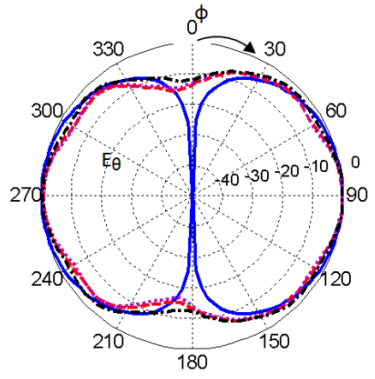


6c

**Figure 6.** The radiation pattern in all planes for different values of ν, at frequency= 1.305GHz

The simulated reflection coefficient, the input impedance as a function of frequency and the radiation patterns in different planes are illustrated in Fig.2, Fig.3 and Fig.4 respectively. The simulated results are calculated by using the FEM and are compared with that calculated by FIT method. Good agreement is obtained. Fig.5 shows the variation of the input impedance and the reflection coefficient versus the frequency at certain values of the squareness parameter ν=2, for A=B=100mm. It is seen that the resonant frequency increases with increasing the value of ν. The resonant input resistance occurs at higher frequencies for higher values of ν. Radiation patterns at the resonant frequency can be calculated. Fig.6 illustrates the Radiation patterns for all planes at f=1.305 GHz for different values of ν. The radiation patterns are omnidirectional in the elevation plane, but they have little changes occurred for different values of ν.

The radiation patterns of the copolarized and cross-polarized fields can be evaluated from $E_\theta$ and $E_\varphi$ components. Using the third definition of Ludwig[16], the copolarized field $E_{copol}$ and cross-polarized field $E_{xpol}$ are expressed as in (3)

$$E_{copol} = E_\theta \cos\varphi - E_\varphi \sin\varphi$$
$$E_{xpol} = E_\theta \sin\varphi + E_\varphi \cos\varphi \quad (3)$$

The copolarized and the cross polarized field components for different values of ν are shown in Fig. 7. As ν increased, the cross polarized field component increased. Fig.8 shows the cross-polarization level, $E_{copol.}/E_{xpol.}$

Figure 9 shows the geometry of CDRA mounted on ground superquadric cylinder structure when A=2B and ν=2. The simulated reflection coefficient and the input impedance as a function of frequency are illustrated in Fig.10 and Fig.11 respectively. The radiation patterns in different planes are displayed in Fig.12. The simulated results are calculated by using the FEM and are compared with that calculated by FIT method. Good agreement is obtained.

As the value of "ν" increased the shape of the disc tends to be rectangular. The computed frequency responses of the real and imaginary parts of the input impedance at different values of ν are shown in Fig.13. The bandwidth getting smaller as the squareness parameter ν increased, the calculated reflection coefficient versus frequency for different values of ν as shown in Fig.14. As shown in Fig.15 the resonance frequency shifts at ahigher value as the squareness parameter ν increases. The copolarized and the cross polarized field components at f=1.32GHz are shown in Fig.16 for different values of the squareness parameter ν. As ν increased the cross polarized field component increased.

The effect of changing the aspect ratio B/A on the reflection coefficient and the input impedance is shown in Fig.17. As B/A decreased the shape of the superquadric cylindrical ground plane tends to be flat and the diffracted field from the edges is increased. The diffracted field may change the resonance frequency and the input impedance of the antenna the resonance frequency is decreased with increasing B/A as shown in Fig.18. The decrease of B/A affects the volume of the CDRA

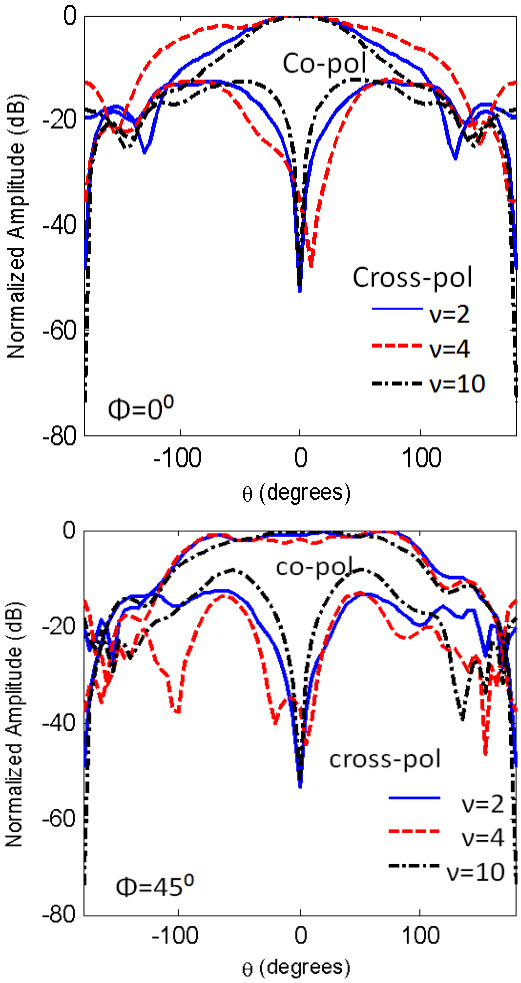


**Figure 7.** The copolarized and the cross polarized field components for different values of ν at frequency= 1.305GHz

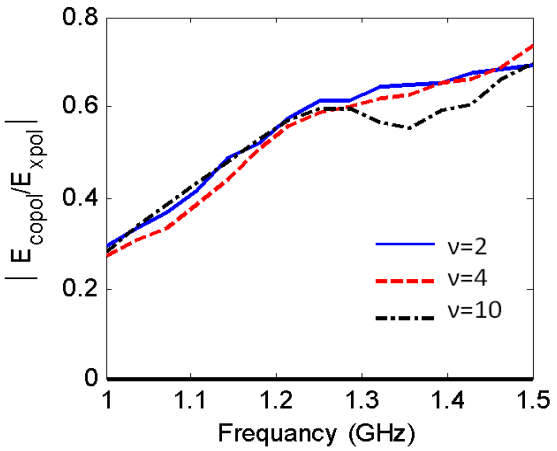


**Figure 8.** Cross-polarization level versus the resonance frequency

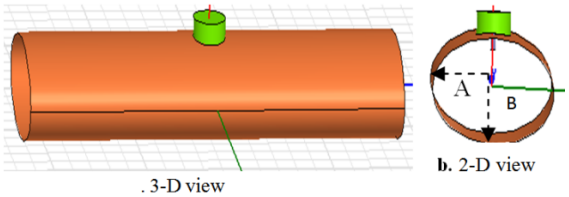


**Figure 9.** The geometry of CDRA mounted on superquadric cylindrical ground plane structure, A= 2B and ν= 2

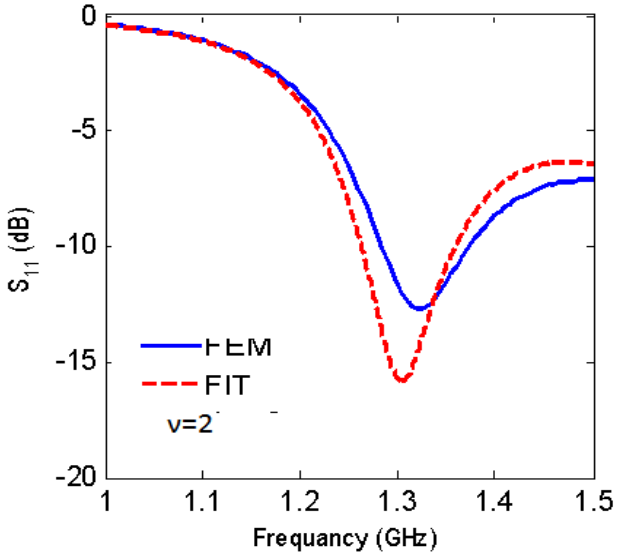


**Figure 10.** Reflection coefficient versus frequency for lg=50cm, A=2B=12.5cm

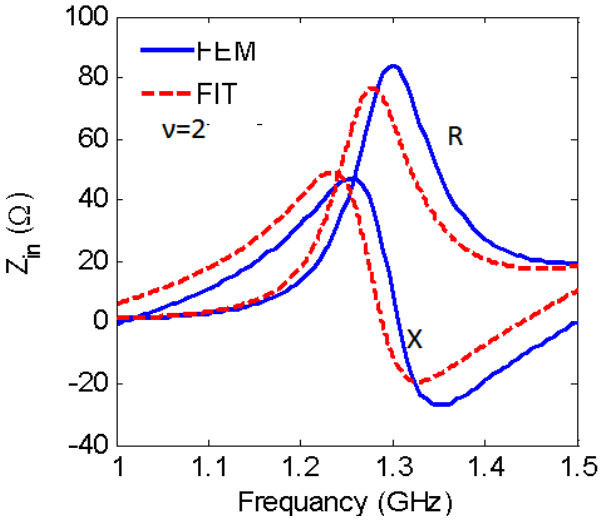


**Figure 11.** Input impedance versus frequency for lg=50cm, A=2B=12.5cm

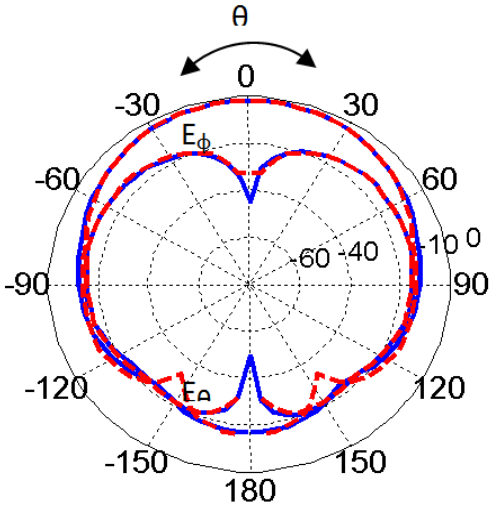


*a*. x-z plane

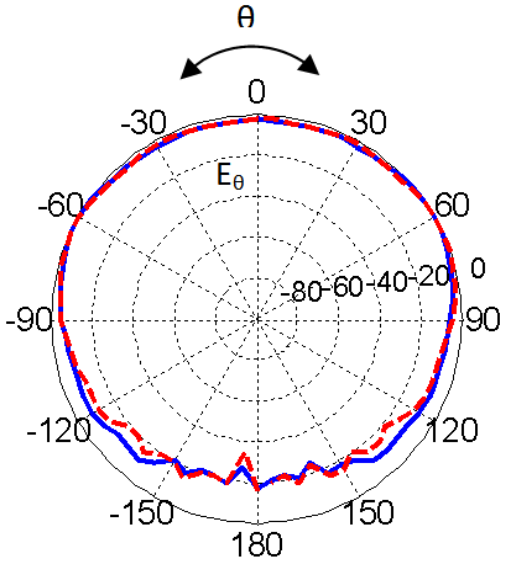


**b**. y-z plane

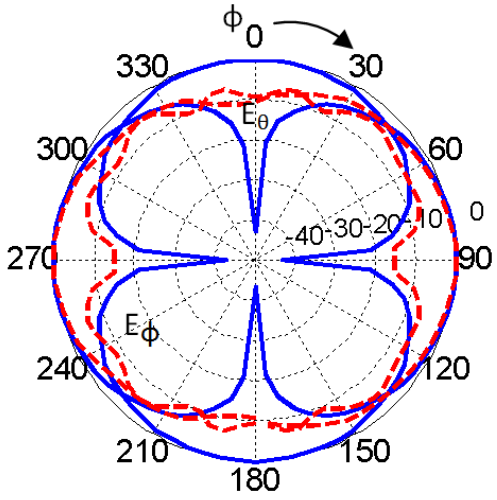


**c**. x-y plane

**Figure 12.** The radiation patterns in all planes at f= 1.32GHz

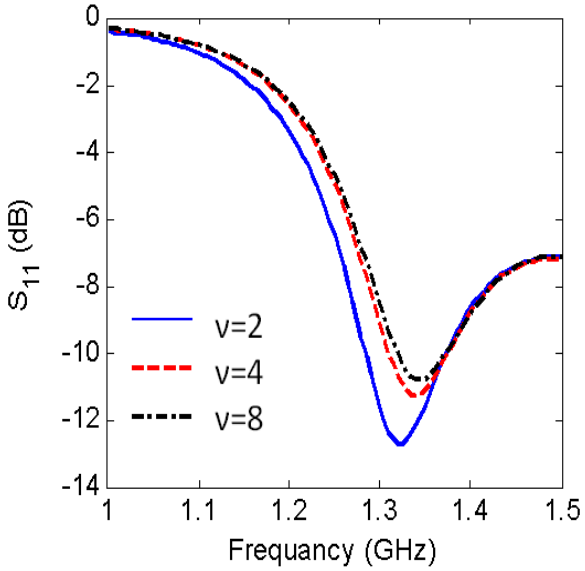


**Figure 13.** Reflection coefficient versus frequency for different values of ν

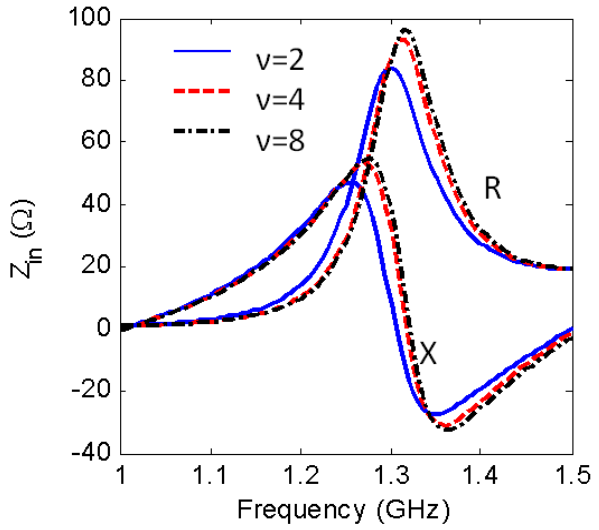


**Figure 14.** The variation of input impedance Versus the frequency for A=2B=12.5cm

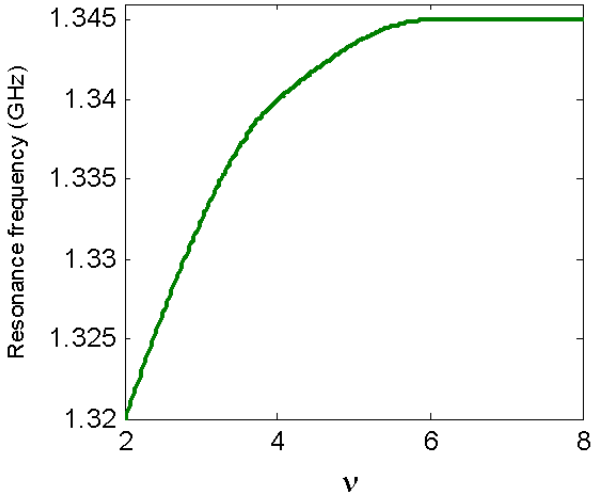


**Figure 15.** The resonance frequency versus the squareness parameter ν, for A=2B=12.5cm

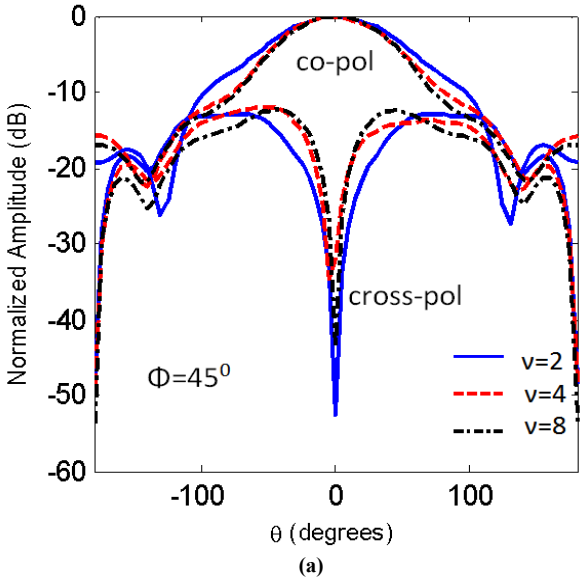


**(a)**

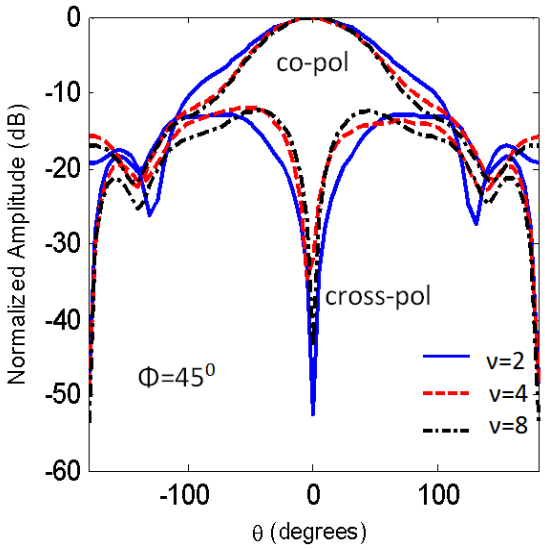


**(b)**

**Figure 16.**The copolarized and the cross polarized field components for different values of ν. at f= 32GHz

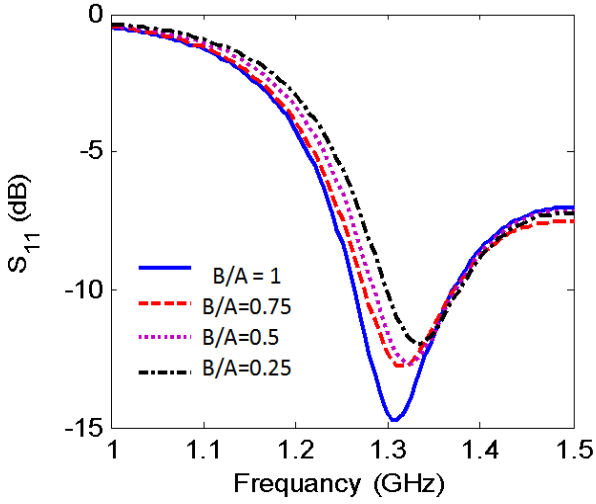


**a.** Reflection coefficient

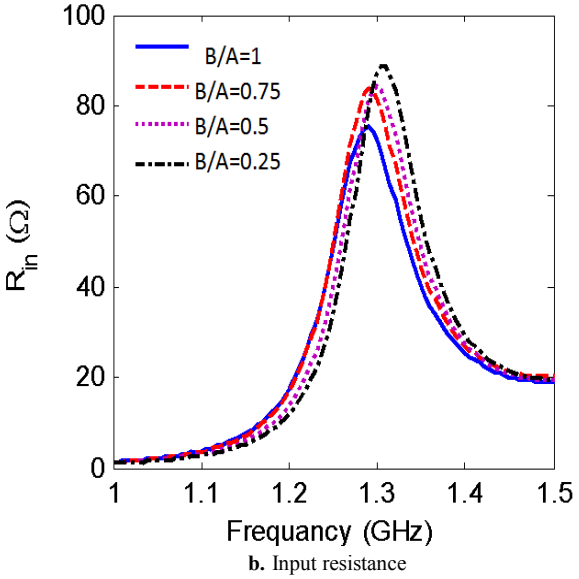


**b.** Input resistance

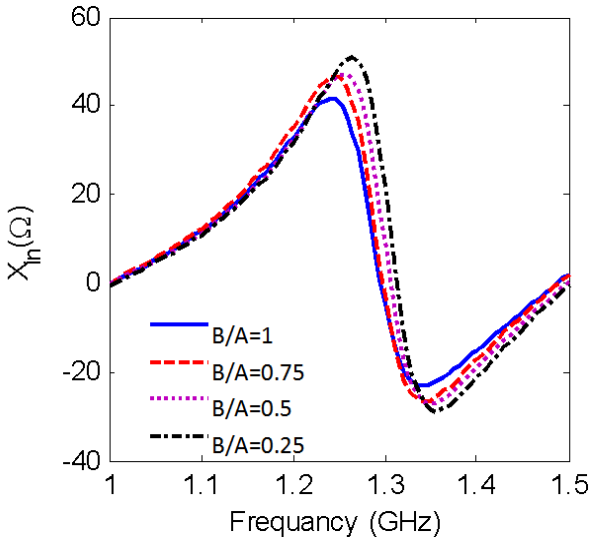


**c.** Input reactance

**Figure 17.** The reflection coefficient and input impedance versus frequency for different values of A/B and ν =2

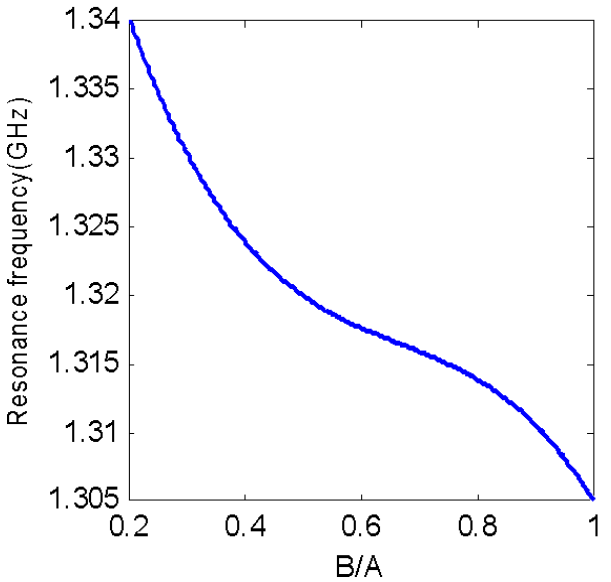


**Figure 18.** The aspect ratio versus resonance frequency, ν = 2, A = 2B = 12.5 cm

## 4. Conclusions

The finite element method and finite integration technique are used to calculate the radiation characteristics of CDRA mounted on superquadric cylindrical body. The effects of changing the value of squareness parameter, ν, on the reflection coefficient, input impedance, resonant frequency, impedance bandwidth, and radiation patterns in different planes are demonstrated. It is seen that as the value of ν increases the resonance frequency increases, the magnitudes of the input resistance, and reactance increase. Also, the cross-polarized field component is increased. The resonance frequency is decreased with increasing the ratio of B/A. However, from Figs. 5,6,7,13,14,15,16,17 and 18, the effect of changing the squareness parameter " ν" from 2 to ∞ and the aspect ratio B/A from 0 to 1 are not causing any significant effect on the characteristics of the CDRA

## REFERENCES

[1] K.M. Luk, and K.W. Leung, Dielectric Resonator Antenna, Research Studies Press, Hertfordshire, UK, 2003.

[2] G. C. Almpanis, Fumeaux, and R. Vahldieck, "The trapezoidal dielectric resonator antenna," IEEE Transactions on Antennas and Propagation, Vol.56, No.9, pp. 2810-2816, September 2008.

[3] G.P. Junker, A.A. Kishk, and A.W. Glisson, "Input impedance of dielectric resonator antenna excited by a coaxial probe," IEEE Transactions on Antennas and Propagation, Vol.42, No.7, pp. 960-966, July 1994.

[4] A.A. Kishk, Y. Yin, and A.W. Glisson, "Conical dielectric resonator antennas foe wideband applications," IEEE Transactions on Antennas and Propagation, Vol.50, No.4, pp. 469-474, April 2002.

[5] B. Li, and K.W. Leung, "On the differentially fed rectangular dielectric resonator antenna," IEEE Transactions on Antennas and Propagation, Vol.56, No.2, pp. 353-359, February 2008.

[6] T.-H. Chang, and J.-F. Kiang, "Sectorial-beam dielectric resonator antenna for WiMAX with bent ground plane," IEEE Transactions on Antennas and Propagation, Vol.57, No.2, pp. 563-572, February 2009.

[7] A. Petosa, Dielectric Resonator Antenna Handbook, Artech House, Inc., Norwood, USA, 2007.

[8] S. H. Zainud-Deen, H. A. Malhat, and K. H. Awadalla," Dielectric resonator antenna mounted on a circular cylindrical ground plane," Progress In Electromagnetics Research B, PIER B, Vol. 19, pp. 427-444, 2010.

[9] S. H. Zainud-Deen, H. A. Malhat, and K. H. Awadalla," Cylindrical dielectric resonator antenna housed in a shallow cavity in a hollow circular cylindrical ground plane." 26rd Applied Computational Electromagnetics Society (ACES) Conference, Tampere, Finland, April 2010.

[10] J. L. Volakis, A. Chatterjee, L. C. Kempel, Finite Element Method for Electromagnetics : Antennas, Microwave Circuits, and Scattering Applications, IEEE Press, Piscataway, NJ, USA, 1998.

[11] Z. Chen, and M. Ney, "The method of weighted residuals: a general approach to deriving time and frequency domain numerical methods" IEEE Antennas and Propag. Magazine, vol. 51, no. 1, pp. 51-70, February 2009.

[12] I. Munteanu1 and T. Weiland, RF & microwave simulation with the finite integration technique – from component to system design, Scientific Computing in Electrical Engineering Mathematics in Industry, Volume 11, Part III, pp. 247-260, 2007.

[13] T. Weiland, "A discretization method for the solution of Maxwell's equations for six-component fields," Electromagnetics and Communications AEÜ, Vol. 31, No. 3, pp. 116-120, March 1977.

[14] Zainud-Deen, S.H., H.A. Malhat, and K.H. Awadalla, "A single-feed cylindrical superquadric dielectric resonator antenna for circular polarization," Progress In Electromagnetic Research, PIER 85, 409-424, 2008.

[15] S. Zhang, C. Zhu, J. K. O. Sin, and P. K. T. Mok, “A novel ultrathin elevated channel low-temperature poly-Si TFT,” IEEE Electron Device Lett., vol. 20, pp. 569–571, Nov. 1999.

[16] A. C. Ludwig, "The definition of crosspolarization," IEEE Transactions on Antennas and Propagation, Vol. 21, pp. 116-119, Jan. 1973.